INTERNATIONAL JOURNAL OF HEAT AND TECHNOLOGY
Vol.33, No.1, 2015

BUOYANCY AND THERMOCAPILLARY DRIVEN FLOWS IN AN OPEN CAVITY WITH BOTTOM HEATING AND SYMMETRICAL COOLING FROM SIDES

N. Nithyadevi*, A. Shamadhani Begum*, C. Udhaya Shankar[O]

*Department of Mathematics, Bharathiar University, Coimbatore-641046, Tamilnadu, India
[O]Department of Electrical and Electronic Engineering, KCT, Coimbatore – 641006, Tamilnadu, India

ABSTRACT

In this study, the effect of thermocapillary and buoyancy driven flows in an open cavity filled with fluid is numerically examined. A physical configuration is encountered where a constant heating element at the bottom wall and cooled from the sidewalls while the top wall can be considered free surface. The length of the heat source is varied from 20 to 100% of the total length of the bottom wall and remaining parts are adiabatic. The governing equations are discretized by finite volume method with power law scheme and solved numerically by SIMPLE algorithm. The effects of dimensionless heat source on flow and heat transfer are studied. The detailed flow pattern and heat transfer characteristics inside the cavity presented in the form of streamlines, isotherms, velocity profiles and average Nusselt number for different values of Grashof number and Marangoni number.

Keywords: Thermocapillary flow; Open cavity; Natural convection; Finite volume method.

1. INTRODUCTION

The study of natural convection in cavities plays a vital role for the transport of heat energy in many engineering applications and naturally occurring process. Most of the works in natural convection are done in different cavities filled with fluids by many authors, especially Ostrach [1], Holmen[2], Taylor [3], Vahl Davis [4] are done with either vertical or horizontal imposed heat flux or temperature difference and Greenspan and Schultz [5] are numerically investigated that natural convection in a cavity with localized heating from below. The present work is motivated by a more general analysis of the heat transfer in electronic equipments. Thermocapillary convection is a fluid motion induced by surface tension gradients on a liquid-gas interface arising from temperature gradients. It is currently a topic of ongoing research interest because of its potential fundamental importance to the understanding of heat transfer in boiling. Rudraiah et al [6] are conducted a numerical study is to understand the effect of magnetic field on the flow driven by the combined mechanism of buoyancy and thermocapillarity in a rectangular open cavity filled with a low Prandtl number fluid (Pr = 0.054).

Natural convection cooling is widely used because of its simplicity, low cost and reliability. Torrance et al. [7] experimentally and Torrance and Rockett [8] numerically studied the convection of air in a vertical cylindrical enclosure, induced by a small hot spot centrally located on the floor. The theoretical results were found to be in an excellent agreement with the experimental ones in the laminar region. Aydin and Yang [9] are numerically investigated that natural convection of air in a two-dimensional, rectangular enclosure with localized heating from below and symmetrical cooling from the sides. They found that the average Nusselt number, $\overline{Nu}$ increase with an increase in the Rayleigh number, Ra, or of the nondimensional heat source thickness, ε. Elatar et al [10] experimentally reported that studied the influence of bottom wall heating on the mean and turbulent flow behaviour in the near wall region during mixed convection. Experimentally and numerically analysis of natural convection in a cavity with Hollow blocks is studied by Stefanizzi et al [11].

Bairi and Oztop [12] surveyed is to quantify the free convective heat transfer that occurs in hemispherical air-filled cavities. Also their results can be used in many engineering domains where hemispherical cavities are used, such as security and safety, solar energy, domestics, building or electronic and electrical devices.

In this paper, we considered the surface tension and natural convection flows in a square cavity having its top boundary open with bottom heating. Localized heating is simulated by a centrally located heat source on the bottom wall and five different dimensionless lengths are considered. The special attention is given to understand the effect of Grashof number and Marangoni number. Applications of this theoretical study will match many experimental heat transfer problems that arise in material manufacturing processes.

2. MATHEMATICAL FORMULATION

Consider a square cavity of length (L) as shown in Figure 1. The lower wall has a centrally located heat source which is assumed to be isothermally heated at a constant temperature θ_h. The sidewalls are isothermally cooled at a constant temperature θ_c. The remaining portion of the bottom and the top wall are thermally insulated. The surface tension on the upper boundary varies linearly with temperature $\sigma = \sigma_0[1-\nu(\theta-\theta_0)]$, where θ_0 - reference temperature, σ_0 - reference surface tension and ν - temperature coefficient of surface tension defined by the equation, $\nu = -\frac{1}{\sigma_0}\frac{\partial\sigma}{\partial\theta}$ and the top surface of the flow domain is assumed to be free. The non-dimensional set of the governing equations are:

$$\frac{\partial U}{\partial X}+\frac{\partial V}{\partial Y}=0 \tag{1}$$

$$\frac{\partial U}{\partial \tau}+U\frac{\partial U}{\partial X}+V\frac{\partial U}{\partial Y}=-\frac{\partial P}{\partial X}+\nabla^2 U \tag{2}$$

$$\frac{\partial V}{\partial \tau}+U\frac{\partial V}{\partial X}+V\frac{\partial V}{\partial Y}=-\frac{\partial P}{\partial Y}+\nabla^2 V+GrT \tag{3}$$

$$\frac{\partial T}{\partial \tau}+U\frac{\partial T}{\partial X}+V\frac{\partial T}{\partial Y}=\frac{1}{\Pr}\nabla^2 T \tag{4}$$

And $$\nabla^2\psi=\frac{\partial U}{\partial Y}-\frac{\partial V}{\partial X} \tag{5}$$

Where $U=\frac{\partial\psi}{\partial Y}$ and $V=-\frac{\partial\psi}{\partial X}$

The non dimensional parameters are defined in the following forms

$$X=\frac{x}{L},\quad Y=\frac{y}{L},\quad U=\frac{uL}{\upsilon},\quad V=\frac{vL}{\upsilon},\quad \tau=\frac{\upsilon t}{L^2},\quad P=\frac{pL^2}{\rho\upsilon^2},$$

$$T=\frac{\theta-\theta_c}{\theta_h-\theta_c},\ \text{with}\quad \theta_h>\theta_c$$

The following nondimensional boundary conditions are obtained:

$$\tau=0:\ U=V=0,\ T=0,\ \text{at}\quad 0\le X\le 1,\qquad 0\le Y\le 1,$$

$$\tau>0:\ U=V=0,\ T=0,\ \text{at}\quad X=0,1,\qquad 0\le Y\le 1,$$

$$U=V=0,\ \frac{\partial T}{\partial Y}=0,\quad \text{at}\ Y=0,\ 0<X<\frac{1-\varepsilon}{2},\frac{1+\varepsilon}{2}<X<1,$$

$$U=V=0,\ T=1,\quad \text{at}\ Y=0,\qquad \frac{1-\varepsilon}{2}\le X\le\frac{1+\varepsilon}{2},$$

$$V=0,\ \frac{\partial U}{\partial Y}=-\frac{Ma}{\Pr}\frac{\partial T}{\partial X},\ \frac{\partial T}{\partial Y}=0,\quad \text{at}\quad Y=1,\qquad 0\le X\le 1,$$

The average Nusselt numbers, $\overline{Nu}$ for the heated portion of the lower wall is given by

$$\overline{Nu}=\int_{\frac{1-\varepsilon}{2}}^{\frac{1+\varepsilon}{2}} Nu\ dX$$

The average Nusselt number, $\overline{Nu}$ for the cooled portion of the left and right wall is given by

$$\overline{Nu}=\frac{1}{2}\left(\int Nu_l dY+\int Nu_r dY\right)$$

where Nu is the local Nusselt number is given by

$$Nu=-\left.\frac{\partial T}{\partial n}\right|_{Y=0 or X=0\&1}$$

$$\mu\frac{\partial u}{\partial y}=\frac{\partial\sigma}{\partial\theta}\frac{\partial\theta}{\partial x}$$

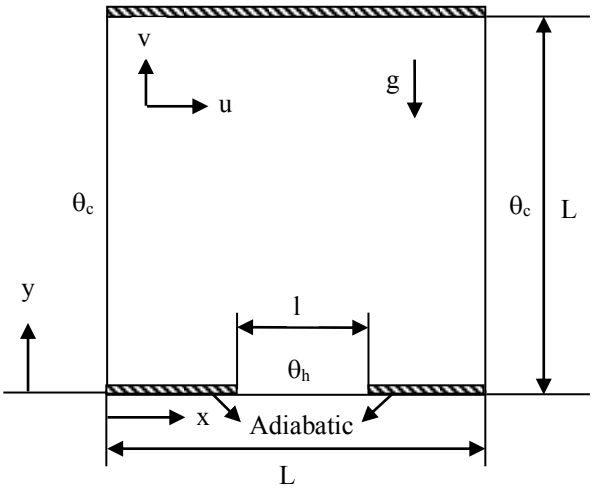

Figure 1. Schematic of the physical system

3. NUMERICAL PROCEDURE

The governing equations along with the boundary conditions are discretised using the finite volume method, with power-law scheme by Patankar [13] and Versteeg and Malasekara [14]. Numerically solved by SIMPLE algorithm for pressure-velocity coupling together with under-relaxation technique. The steady state solution is obtained when the following convergence criteria for temperature and stream function have been met.

$$\left|\frac{\phi_{n+1}(i,j)-\phi_n(i,j)}{\phi_{n+1}(i,j)}\right|\le 10^{-5}$$

The time step is taken to 10^{-5} for all computations. Uniform staggered grid system is employed in this presentation. The numerical solutions are presented by using 151×151 grid points. As increasing grid size from 151×151 to 181×181 there is no noticeable changes in the average heat transfer. Therefore, 151×151 grid size is approved to be sufficient to resolve the velocity and temperature fields for the related case.

4. VALIDATION OF CODE

Table 1 depicts the comparison of average Nusselt number for different Rayleigh number in an open cavity with Pr=0.7. The results are compared with the solutions of Vahl Davis [15], Tasnim [16], Ambarita[17] . The results are found to be good agreement with these solutions. Finally, the model is tested against the work of Sharif and Mohammad [18] for the case of $10^3 \le Gr \le 10^6$ and ε=0.2 &

0.4 in Table 2. As increasing the Grashof number, the error percentage is decreases. This validation makes a good confidence in the present numerical model to deal with the same square configuration problem.

Table 1. Comparison of average Nusselt Number for different Rayleigh number in a square cavity with Pr = 0.71

Reference	$\overline{Nu}$				
	Ra = 10^4	**Ra = 10^5**	**Ra = 10^6**	**Ra = 10^7**	**Ra = 10^8**
Vahl Davis [15]	2.234	4.51	8.798	-	-
Tasnim [16]	2.244	4.5236	8.8554	-	-
Ambarita [17]	2.228	4.514	8.804	16.52	30.48
Present	2.247	4.542	8.850	16.92	31.56

Table 2. Comparison of average Nusselt number for different Grashof number and Pr=0.71

Gr	$\overline{Nu}$			
	Sharif and Mohammad [18] ε=0.2	**Present**	**Sharif and Mohammad [18] ε=0.4**	**Present**
10^3	5.926608	5.908235	4.084653	4.028635
10^4	5.946352	5.913524	4.132314	4.101235
10^5	7.124055	7.100892	6.057670	6.023842
10^6	11.34151	11.318235	10.51224	10.48538

5. RESULTS AND DISCUSSION

Heat distribution and fluid flow are depicted in Figure 2 in the form of isotherms and streamlines respectively for different dimensionless heat source lengths ($1/5 \leq \varepsilon \leq 5/5$), Ma=100, Gr=$10^5$. In the beginning, the basic flow structure has two symmetrical counter rotating cells are exists about the vertical centreline. Due to the symmetrical boundary conditions on the vertical walls, the high buoyancy force gives a pair of flow structure inside the cavity. As ε soars, the streamlines are gathering towards the cold walls and the gentle increase in flow strength. An increasing trend of non-dimensional heater length produces larger temperature distribution in the entire zone of cavity and they are dense near the left and right corners of bottom wall. When the heater is stretching along the whole width of the bottom wall (ε = 5/5) pointing that the conduction dominated heat transfer mechanism over the heater surface. Figure 3 shows the streamlines and isotherm contours for various non-dimensional size of the isothermal heat sources ε=1/5,2/5,..5/5 and Ma=1000, Gr=10^5. For ε=1/5, there is a formation of strong primary eddies at the bottom wall and weak secondary eddies at the top of cavity. By increasing heat source length, the effect on secondary eddies increases and pushed downwards. As ε increases, the flow rate increases and the magnitudes of the temperature gradient increases. When we compare the Figures 2 and 3, the Ma from 100 to 1000, a foremost secondary eddies are appeared at the top of cavity due to the effect of thermocapillary force. But in isotherms, the convection mode is maintained. In Figure 4 the steady state streamlines and isotherms are plotted to show the effect of different Ma and Gr=10^5, ε=2/5, Pr=0.054. This figure reveals the result of surface tension effect ($0 \leq Ma \leq 1000$) in an opened cavity and therefore a prominent secondary eddy is observed at the top due to the interface of Marangoni effect. On the whole, as increasing the surface tension force, the buoyancy force is dominated by the thermocapillary force. The same results are observed by the effect of surface tension force is shown in Figure 5. The same parameters except the heat source length ε=4/5 is taken. By increasing ε from 2/5 to 4/5 from

the Figures 4 and 5, the flow rate is increases and thus convection gets strengthened.

In order to have a better understanding of the flow behaviour with in cavity, the bidirectional velocity profiles are plotted at the mid section of the cavity for various values of ε and Ma in Figures 6 & 7. Figure 6 represents the mid-height vertical velocity at the middle of cavity for different ε, Ma=100, Pr=0.054 and Gr=10^5. A Sinusoidal behaviour is observed for the distribution of the mid-height vertical velocity profile, as it is irregular for the various parameter of heater length, whilst it is interesting that the flow reaches its maximum point in the middle of the enclosure and returns to attain its mid value at the edges. This is due to the high values of the stream function with two symmetrical counter rotating cells, symmetric about the vertical centre line in the enclosure. The peak velocity deflection near the corner move towards the side wall with high surface tension force Ma=100 &1000 in Figure 7. The depression on the flow becomes flatten for low Marangoni number with ε=4/5. Figure 8 is plotted for both hot and cold wall to show the effect of ε on different Grashof number over the Average Nusselt Number and Pr=0.054, Ma=100. In the hot wall, for Gr≤10^5 the heat transfer rate is almost invariant. When Gr>10^5, the buoyancy aids more and more in the heat transfer process which results in more rapid increase of $\overline{Nu}$. For the cold wall, the changes in results are almost same and identical to the hot wall. Hence for the small length of the heat sources (1/5, 2/5) the heat transfer is purely conduction. Further increasing ε, the average Nusselt number is constant until Gr=10^5. But it increases for higher Grashof number Gr=10^6.

The average Nusselt number is affected by the surface tension force Ma in a different way as seen in the Figure 9. Here the heat transfer rate is calculated for both hot and cold wall. The effect of surface tension force on the flow is more evident from these profiles as the heat transfer rate changes substantially when Ma is changed. For ε=2/5 for both hot and cold wall, there is no changes as Ma increases. While changing ε=4/5, $\overline{Nu}$ elevates in a small region of the left wall of the cavity and then it starts to decrease smoothly for Gr=10^5. The time history of average Nusselt number for different heater length ε and Ma = 100, Ha = 50, Gr = 10^5 is depicted in Figure 10. At the initial time, the average Nusselt number drops for the increasing heater length and then it obviously attains the steady state for the hot wall. This is due to changing the mode of heat transfer from conduction to high convection. But in the cold wall, the $\overline{Nu}$ increases, passes through the maximum and reaches the steady state.

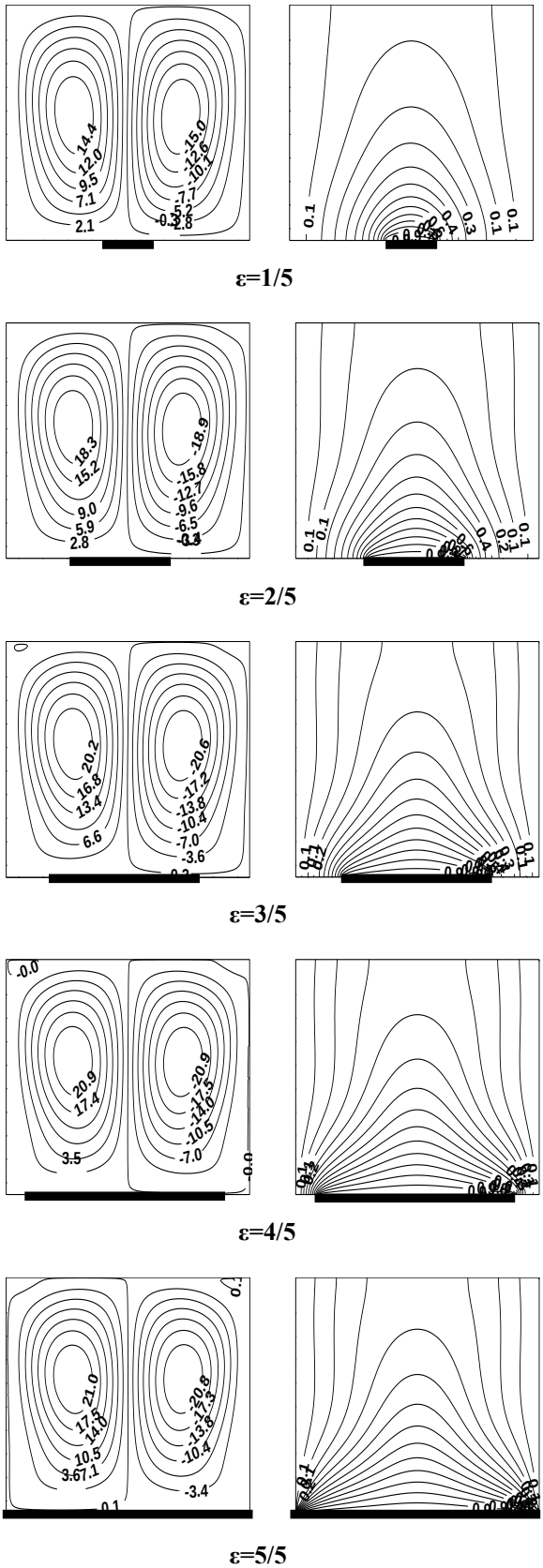

Figure 2. Steady state Streamlines and Isotherms for different heating locations and Ma=100, Gr = 10^5

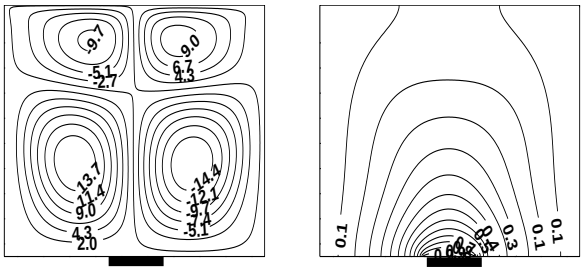

ε=1/5

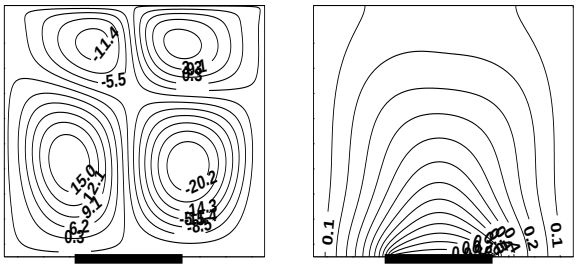

ε=2/5

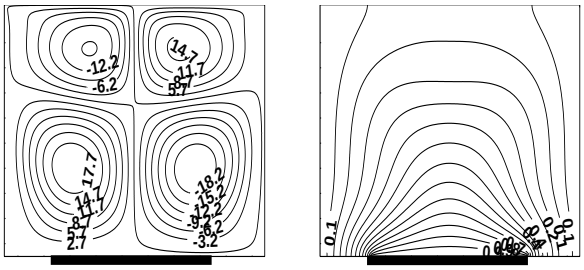

ε=3/5

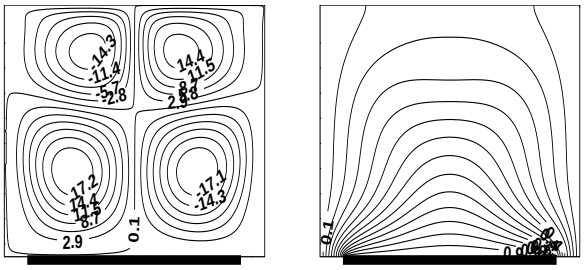

ε=4/5

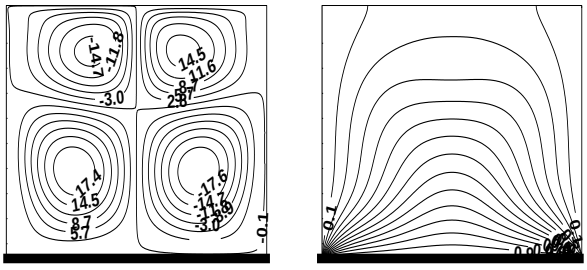

ε=5/5

Figure 3. Steady state Streamlines and Isotherms for different heating locations and Ma = 1000, Gr = 10^5

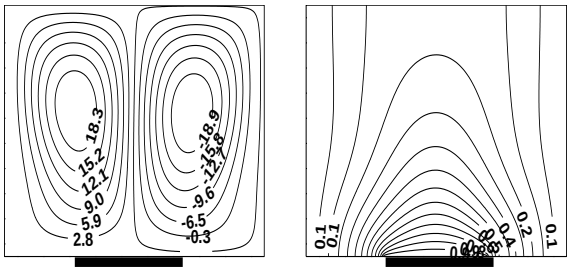

Ma=0

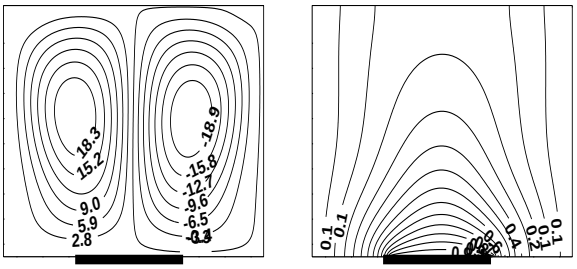

Ma=100

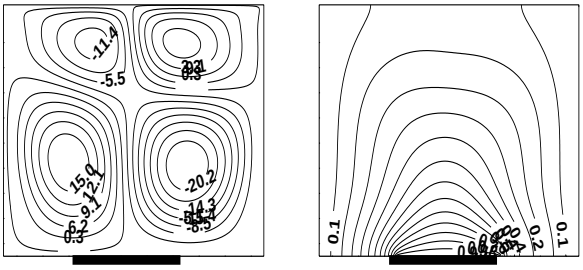

Ma=1000

Figure 4. Steady state Streamlines and Isotherms for different Ma,
Gr = 10^5 and ε = 2/5

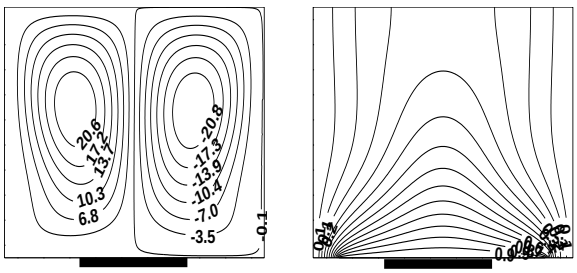

Ma=0

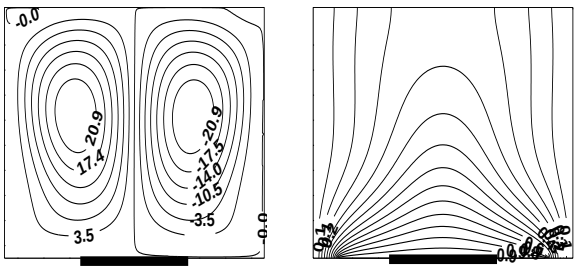

Ma=100

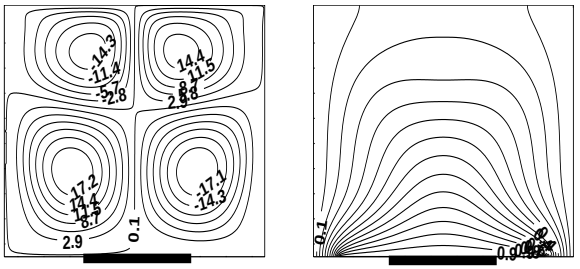

Ma=1000

Figure 5. Steady state Streamlines and Isotherms for Different Ma,
Gr = 10^5 and ε = 4/5

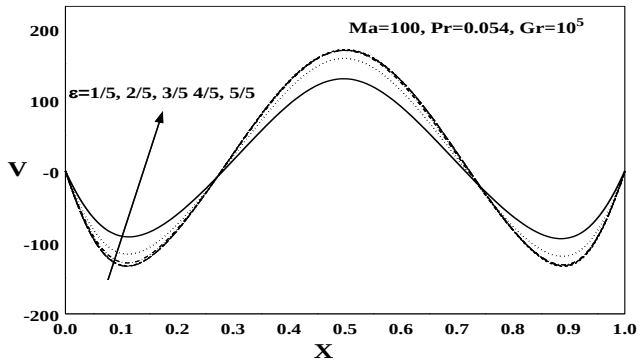

Figure 6. Mid-height Vertical velocity at the middle of the cavity for different ε and Ma=100, Pr=0.054 & Gr =10^5

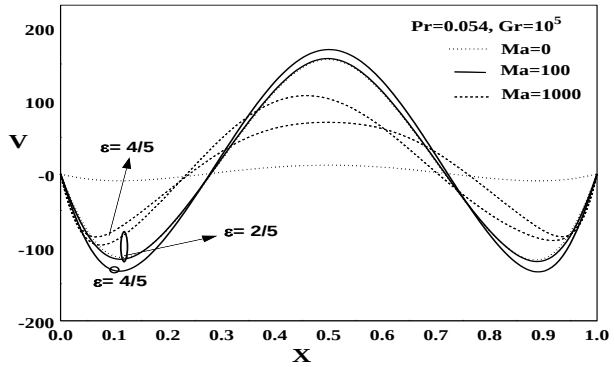

Figure 7. Mid-height Vertical velocity at the middle of the cavity for different Ma and Pr=0.054, Gr=10^5

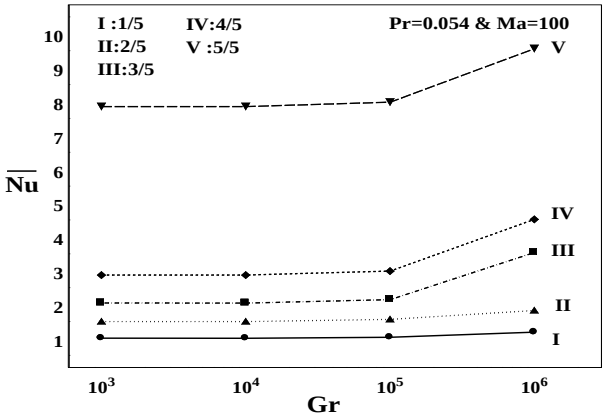

a) Hot Wall

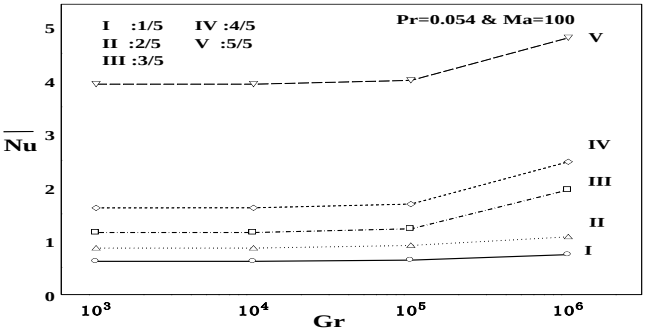

b) Cold Wall

Figure 8. Average Nusselt number vs Gr for different heating location, Pr=0.054 and Ma=100

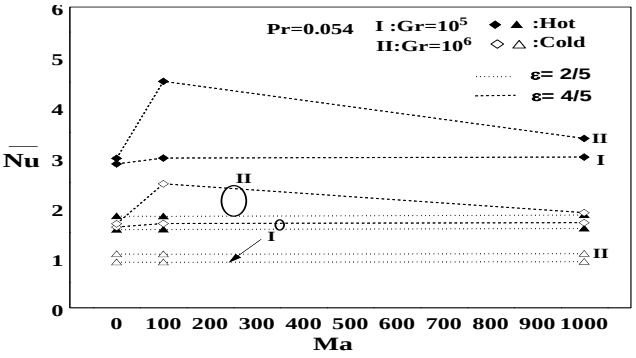

Figure 9. Average Nusselt number vs Marangoni number for different Gr, ε=2/5 & 4/5, Pr=0.054

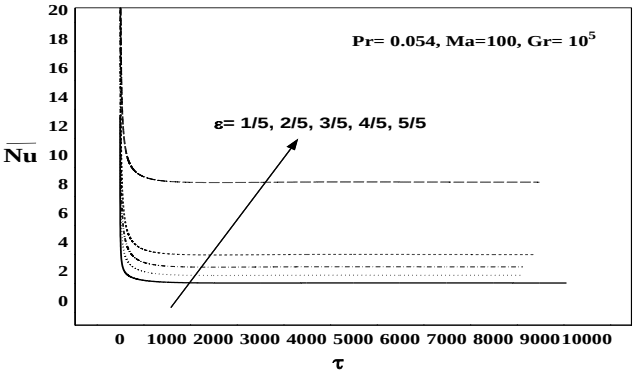

a) Hot Wall

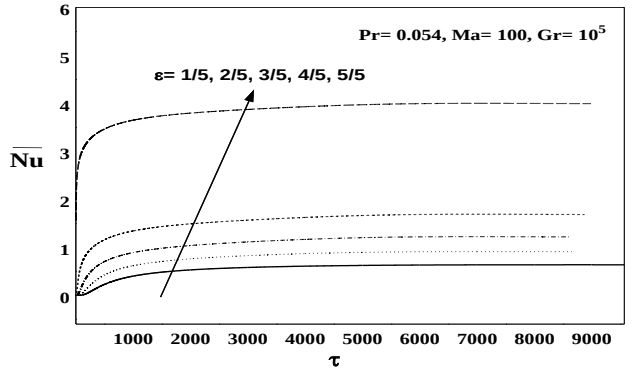

b) Cold Wall

Figure 10. Time history for different ε, Pr=0.054, Ma=100 & Gr=10^5

6. CONCLUSION

The results of a numerical study of buoyancy and thermocapillary-driven flows in a two-dimensional free top surface cavity with constant heating at the bottom wall and isothermal cooling from the side walls are analyzed and presented. The most important parameters are Grashof number, Marangoni number and dimensionless heat source. The flow and temperature fields are symmetrical about the mid length of the cavity due to the symmetrical boundary conditions in the vertical direction. The following conclusion can be drawn from this study.

(a) By varying length of the heat sources with different Marangoni number, the secondary eddies are formed due to thermocapillary force.

(b) The average Nusselt number increases for increasing Grashof number. Increasing ε enhances the heat transfer, especially for higher values of Gr.

(c) Variation of average Nusselt number with τ varies and reaches steady state by two driving mechanism acting on the flow.

REFERENCES

1. S. Ostrach, Natural Convection in Enclosures, *Advans. Heat Transfer*, vol. 8, pp. 161-227, 1972.
2. J. P. Holmen, Heat Transfer, McGraw-Hill, Singapore, 1986.
3. C. Taylor and A. Z. Ijam, A Finite Element Numerical Solution of Natural Convection in Enclosed Cavities, Comput. *Methods Appl. Mach. Engg.*, vol. 19, pp. 429-446, 1979.
4. G. Vahl Davis, Laminar Natural Convection in an Enclosed Rectangular Cavity, *Int. J. Heat Mass Transfer*, vol. 11, pp. 1675-1693, 1968.
5. D. Greenspan and D. Schultz, Natural Convection in an Enclosure with Localized Heating from Below, *Comput. Methods Appl. Mach. Engg.*, vol. 3, pp. 1-10, 1974.
6. N. Rudraiah, M. Venkatachalappa and C. K. Subbaraya, Combined Surface Tension and Buoyancy-driven Convection in a Rectangular Open Cavity in the Presence of Magnetic Field, *Int.J. Nonlinear Mechanics*, vol. 30(5), pp. 759-770, 1995.
7. K. E. Torrence, L. Orloff and J. A. Rockett, Experiments on Natural Convection in Enclosures with Localized Heating from Below, *J.Fluid Mech*, vol. 36, pp. 21-31, 1969.
8. K. E. Torrence and J. A. Rockett, Numerical Study on Natural Convection in an Enclosure with Localized Heating from Below, *J. Fluid Mech*, vol. 36, pp.33-54, 1969.
9. O. Aydin and W. J. Yang, Natural Convection in Enclosures with Localized Heating from Below and Symmetrical Cooling from Sides, *Int. Journal of numerical Methods for heat & Fluid Flow*, vol. 10, pp. 518-529, 2000.
10. A. Elatar and K. Siddique, The Influence of Bottom Wall Heating on the Mean and Turbulent Flow Behaviour in the Near Wall Region During Mixed Convection, *Int. J. Thermal Sciences*, vol. 77, pp. 233-243, 2014.
11. P. Stefanizzi, A. Lippolis and S. Liuzzi, Experimental and Numerical Analysis of Heat Transfer in the Cavities of Hollow Blocks, *Int. J. Heat Technology*, vol. 31, pp. 149-154, 2013.
12. A. Bairi and H. F. Oztop, Free Convection in Inclined Hemispherical Cavities with Dome Faced Downwards. Nu-Ra relationships for Disk Submitted to Constant Heat Flux, *Int. J. Heat Mass Transfer*, vol. 78, pp. 481-487, 2014.
13. G. Vahl Davis, Natural Convection of Air in a Square Cavity; A Bench Mark Numerical Solution, *Int. J. Numerical Methods in Fluids*, vol. 3, pp. 249-264, 1983.
14. S. H. Tasnim and M. R. Collins, Numerical Analysis of Heat Transfer in a Square Cavity with the Baffle on the Hot Wall, *Int. Comm. Heat Mass Transfer*, vol. 31, pp. 639-650, 2004.
15. H. Ambarita, K. Kishinami, M. Daimaruya, T. Saitoh, S. Takahashi and J. Suzuki, Laminar Natural Convection Heat Transfer in an Air filled square cavity with two Insulated Baffles attached to its Horizontal Walls, *Thermal Science and Engineering*, vol. 14, pp. 35-46, 2006.
16. M. A. R. Sharif and T. R. Mohammed, Natural Convection in Cavities with Constant Flux Heating at the Bottom Wall and Isothermal Cooling from the Side Walls, *Int. Journal of Thermal Sciences*, vol. 44, pp. 865-878, 2005.
17. S. V. Patankar, Numerical Heat Transfer and Fluid Flow, Hemispahere Publishing Corporation, USA, 2004.
18. H. K. Versteeg and W. Malasekara, An Introduction to Computational Fluid Dynamics: The Finite Volume Method, Longman, England, 1998.

NOMENCLATURE

g	=	Gravitational acceleration (m/sec^2)
Gr	=	Grashof number$(g\beta(\theta_h-\theta_c)L^3)/\nu^2$
k	=	Thermal conductivity (W/mK)
L	=	Length of the square cavity (m)
Ma	=	Marangoni number $(\partial\sigma/\partial\theta)((\theta_h-\theta_c)/\mu\alpha)L$
Nu	=	Local Nusselt number
$\overline{Nu}$	=	Average Nusselt number
p	=	Pressure (Pa)
P	=	Non-dimensional Pressure
Pr	=	Prandtl number (ν/α)
T	=	Temperature (K)
u,v	=	Velocity components (m/s)
U,V	=	Dimensionless velocity components
x,y	=	Cartesian coordinates (m)
X,Y	=	Dimensionless Cartesian coordinate

Greek Symbols

α	=	Thermal diffusivity (m^2/sec)
β	=	Coefficient of thermal expansion (1/K)
ε	=	Dimensionless length of heatsource(l/L)
θ	=	Dimensionless temperature
μ	=	Dynamic viscosity (Ns/m^2)
ν	=	Kinematics viscosity (m^2/s)
ρ	=	Density of the working fluid (kg/m^3)
σ	=	Surface tension
τ	=	Dimensionless time
ψ	=	Stream function

Subscripts

c	=	Cold wall
h	=	Hot wall
0	=	Reference state